Bull. Spec. Astrophys. Obs., 1998, 46, 110–117

Spectroscopy of halo stars

S. V. Ermakov, V. G. Klochkova

Special Astrophysical Observatory of the Russian AS, Nizhnij Arkhyz 357147, Russia

Received October 6, 1998; accepted October 29, 1998.

Abstract. This work is the next step of our spectroscopic research of stars with large proper motions (Klochkova et al., 1996; Klochkova, Panchuk, 1996). We present new data for 12 stars from the lists of Carney et al. (1994) and Bartkevičius (1980). Spectroscopic study of the sample of stars from these lists is carried out at the 6 m telescope for the purpose of detailed investigation of their chemical composition as well as determination of parameters (effective temperature, surface gravity, microturbulent velocity, metallicity and radial velocity). The use of echelle spectra allowed the model atmosphere method to be applied both for the determination of chemical element abundances and fundamental parameters. In so doing we used the grid of Kurucz's (1993) models. Our approach is distinguished by using homogeneous high quality material (S/N > 100 and spectral resolution R > 25000) in a wide range of wavelengths and application of a common technique for reduction of spectra and quantitative analysis of data. The atmospheric parameters of the stars under study lie within the limits: 4300 K < $T_{\rm eff}$ < 6900 K; 0 < log g < 5; −2.9 < [Fe/H] < +0.3.

Key words: stars: abundances – stars: fundamental parameters – stars: population II

1. Introduction

Determination of chemical element abundances of stars of different populations (halo, disk) plays the basic role in the understanding of chemical evolution of our Galaxy. The chemical composition of **halo** stars is primarily of interest because it carries information on the processes of enrichment in chemical elements at early stages of Galaxy formation, including the contribution of some nucleosynthesis processes to the observed abundance of elements in the solar system. From this point of view, it is of the greatest interest to study chemical composition of low-metallicity **unevolved** stars, i.e. the stars that have had no time to come off the main sequence — halo subdwarfs. The most attractive halo objects in this case are globular clusters because the luminosities and evolutionary stages of cluster members can be determined with sufficient reliability. Nearby field subdwarfs, however, have a number of advantages comparing with globular clusters: firstly, to observations are available field subdwarfs well brighter as compared to stars in the nearest globular clusters, which makes it possible to acquire spectra of fairly high quality; secondly, there are field stars showing essentially lower metallicities in comparison with globular clusters, which means that we can investigate into the earlier epochs of halo evolution.

2. Observations and primary reduction of spectra

2.1. Echelle spectroscopy

We obtained all the spectra at the 6 m telescope with the echelle spectrometers LYNX (Klochkova, 1998) and PFES (Panchuk et al., 1998) equipped with a 1040×1160 pixels CCD. The observations were carried out in the spectral ranges 5000 – 7200 ÅÅ and 5500 – 8700 ÅÅ. To take into account of cosmic particles, for each of the objects at least two echelle spectra were recorded during the night. To distinquish the absorption lines of the Earth's atmosphere, a fast-rotating star (HR 4687) was observed every night. Apart from the principal 12 stars two standards, HD 122563 and α CMi, were observed to test the technique. A thorium–argon spectrum was used as the comparison one, which was recorded a few times during each night.

The processing of two-dimensional echelle frames (dark frame subtraction, removal of cosmic particles' traces, wavelength calibration, as well as extraction of one-dimensional echelle orders) was performed in the system ESO–MIDAS. Further reduction of one-dimensional linearized spectra (plotting the continuum, equivalent widths and radial velocities measurement) was done using the programme DECH20 (Galazutdinov, 1992). As an illustration, in Fig. 1 is presented a portion of the spectrum around the line

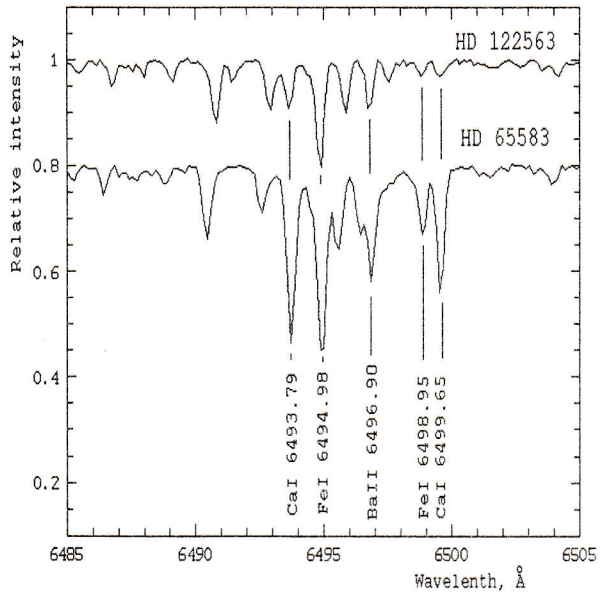

Figure 1: *A portion of the spectrum about the line BaII* λ 6496 Å *for two stars of different metallicity:* [Fe/H] $= -2.63$ *for HD 122563 and* [Fe/H] $= -0.15$ *for HD 65583.*

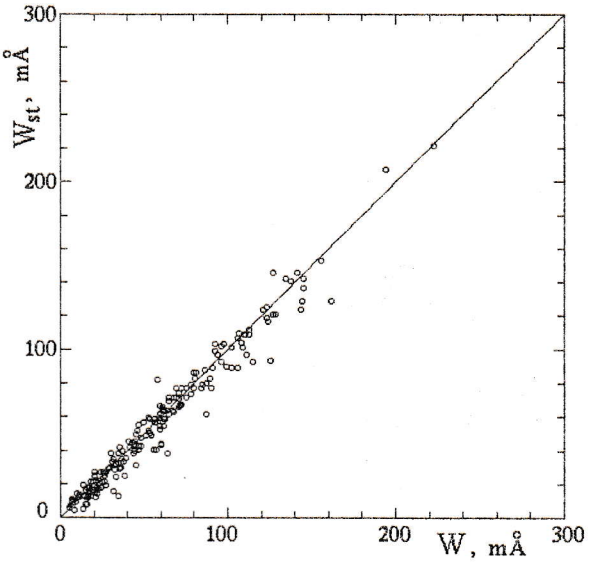

Figure 2: *Comparison of the equivalent widths W we measured in the* α *CMi spectrum with the data from Steffen (1985).*

BaII λ 6496 for two stars of different metallicities.

2.2. Equivalent width measurement

Since most of our programme stars were rather metal-deficient and the observations were conducted in a relatively red part of the spectrum, the continuum placement was not difficult (except for the H_α line region, and also the portions with a great number of telluric absorption lines; in the orders where the continuum could not be drawn reliably enough, the equivalent widths were not measured). The list of lines and oscillators strengths used in the computation of element abundances and determination of fundamental parameters of stellar atmospheres is presented in the paper by Klochkova et al. (1996). We selected minimum blended lines and in the calculations we used the lines with the equivalent width W $<$ 100 mÅ, as a rule. For checking a comparison was made with a synthetic spectrum computed with the corresponding parameters of stellar atmospheres and also with the spectrum of a hot fast-rotating star. The spectral data obtained at the 6 m telescope allowed us to measure equivalent widths to an accuracy of 2–4 mÅ. For a considerable part of echelle spectra the overlapping of orders, especially in the blue region, made it possible to measure the lines twice, which also improved the accuracy of equivalent width determination. Our measures are compared with the data of other authors for α CMi in Fig. 2. As can be seen from the figure, there is no systematic trend for the equivalent widths we used.

3. Determination of atmospheric parameters

To determine parameters of the models (effective temperature $T_{\rm eff}$, surface gravity $\log g$, microturbulent velocity ξ_t and chemical element abundances), we applied the model atmosphere method and used Kurucz's (1993) grid of stellar atmosphere models. Given a large enough set of line equivalent widths of neutral iron FeI even for the most low-metallicity stars, we estimated $T_{\rm eff}$ from the condition that the neutral iron abundance is independent on the excitation potential of the given line; the surface gravity $\log g$ — from the condition of ionization balance for the iron atoms, and the microturbulent velocity ξ_t — from the assumption that the iron abundance is independent on the line equivalent width. In so doing, we used single unblended lines whose equivalent widths lie within the interval 10 $<$ W $<$ 100 mÅ. Taking α CMi as an example, Figures 3 and 4 illustrate the process of determining the atmosphere parameters. α CMi, which is one of the stars whose parameters have repeatedly been determined by different methods, shows clearly the difference in effective temperatures found using different techniques: from 6500 K by photometry to 6750–6900 K by spectroscopy. This point has been discussed in more detail by Steffen (1985) and Klochkova, Panchuk (1996).

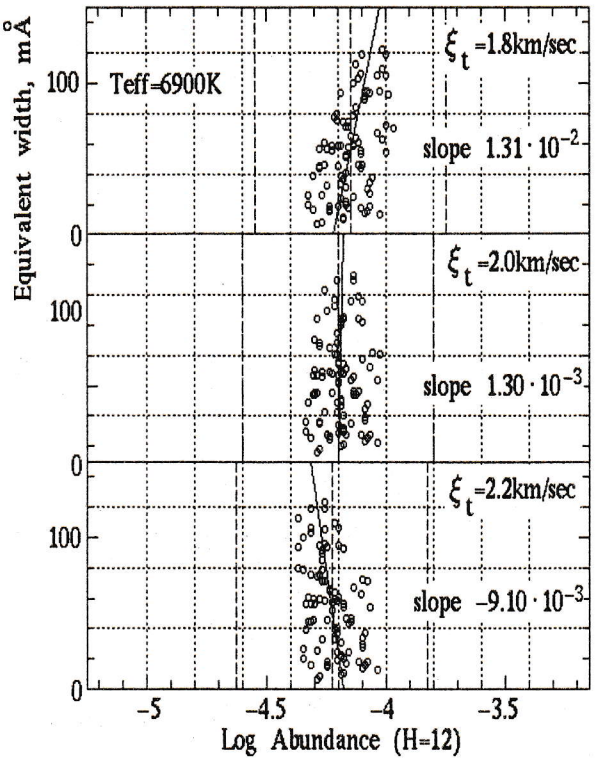

Figure 3: *Microturbulent velocity determination for α CMi.*

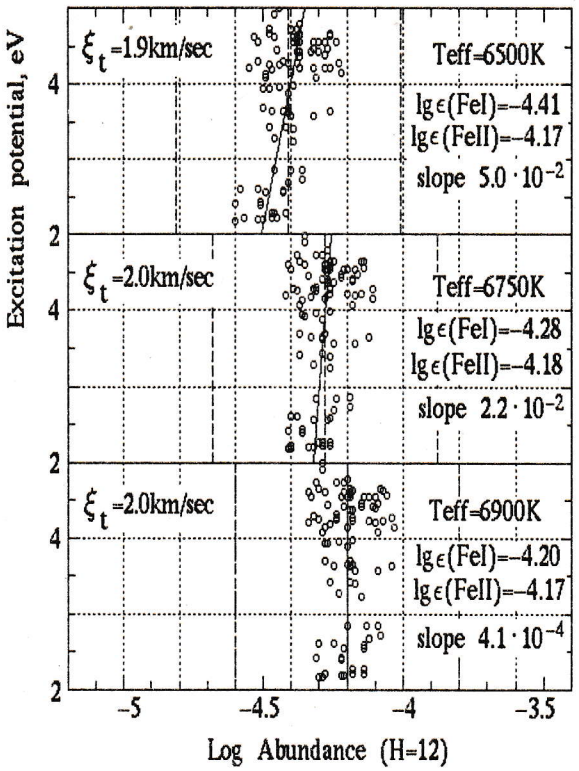

Figure 4: *Effective temperature determination for α CMi.*

The model atmosphere parameters that we have determined for the programme stars are listed in Table 1. From the photometry data the greater part of our objects should be referred to halo subdwarfs. However, the atmospheric parameters estimated by spectroscopy suggest, as can be seen from Table 1, that only a small part of the sample stars can be referred to unevolved stars. Besides, from our results the metallicity is generally higher than that obtained from photometry. Thus, the original task of investigation of unevolved halo stars has transformed into investigation of a sample of stars of a wider range as to their parameters. The absolute magnitudes M_v of the stars estimated from *Hipparcos* parallaxes are given in Table 1 and plotted with error bars vs. values of $\log g$ in Fig. 5.

4. Discussion

When explaining the observed relationships of element abundances and modelling chemical evolution of the Galaxy, three basic mechanisms of synthesis of elements in the process of evolution of stars are generally considered (see Wheeler et al., 1989 and references therein).

1. Massive ($M \geq 8 M_\odot$) short-lived stars, which enrich the interstellar medium with the nucleosynthesis products through the stellar wind at the final stages of evolution during the second-type supernovae (SNII) outbursts, are considered to be the main source of α-process elements and light elements with odd Z (Na and Al) (Truran, 1984; Woosley and Weaver, 1986).

2. Supernovae of type Ia are suggested to be the main source of iron group elements. This mechanism of element synthesis is actuated later than the former and this can explain the decrease in α-process elements [α/Fe] from 0.4 for halo stars to 0 for stars of about solar metallicity (Edvardsson et al., 1993; Truran, 1984; Woosley and Weaver, 1986).

3. Asymptotic giant branch stars are the supplier of s-process elements synthesized in the shell source and swept into the interstellar medium by the stellar wind and superwind when planetary nebulae form. The masses of such stars do not exceed $8 M_\odot$ (Iben, 1983).

The final results of calculation of chemical element abundances with respect to solar (averaged over all measured lines) obtained for the programme stars in

Table 1: *The main parameters of stars studied*

Star	V	T_{eff}, K	M_V*	log g	ξ_t, km/s	[Fe/H]	V_r, km/s
G 30-52	8.59	5025	5.40	2.5	3.2	-0.60	21.3
G 126-62	9.47	6640	4.09	4.55	0.9	-0.93	-288.7
G 170-47	8.95	5000	2.10	1.9	1.1	-2.47	-282.5
G 231-52	10.34	5750	6.27	4.4	2.1	-1.49	-244.6
G 245-32	9.95	6725	3.99	4.65	0.3	-0.72	-271.0
HD 65583	6.94	5800	5.84	5.0	1.1	-0.20	15.6
HD 88609	8.61	4325	-2.41	0.0	2.3	-2.82	-36.2
HD 175305	7.20	5000	0.46	2.2	1.2	-1.35	-181
BD 09°3223	9.27	5900	0.62	2.6	3.2	-1.53	67.0
BD 11°2998	9.2	5625	1.62	2.4	1.8	-0.88	50.2
BD 17°3248	9.37	5590	2.16	2.4	1.1	-1.15	-145.6
BD 23°3912	8.88	5880	3.75	3.6	1.4	-1.22	-115.4
HD 122563	6.20	4395	-0.94	0.0	1.8	-2.77	-30
α CMi	0.34	6900	2.68	4.0	2.0	+0.30	-3.5

*- absolute magnitudes M_V were calculated using *Hipparcos* parallaxes

the form

$$[X/Fe] = \{\log\epsilon(X) - \log\epsilon(Fe)\} - \{\log\epsilon(X)_\odot - \log\epsilon(Fe)_\odot\}$$

are tabulated in Table 2. The abundance determination errors and the number of lines used in the analysis are given in brackets. To calculate the values [X/Fe] we used the solar chemical composition from the paper by Grevesse et al. (1996). In Figures 6, 8, 9 are shown the relative abundances [X/Fe] of some elements and groups of elements as a function of metallicity. Apart from the data obtained in the present work the data of Klochkova et al. (1996) are also considered for this paper in the continuation of the latter and the technique of determination of the parameters and abundances is the same. In all the figures the circles denote the element abundance for stars with $\log g \geq 3$, while the squares indicate stars with $\log g < 3$. The abundances of some elements and groups of elements are discussed below.

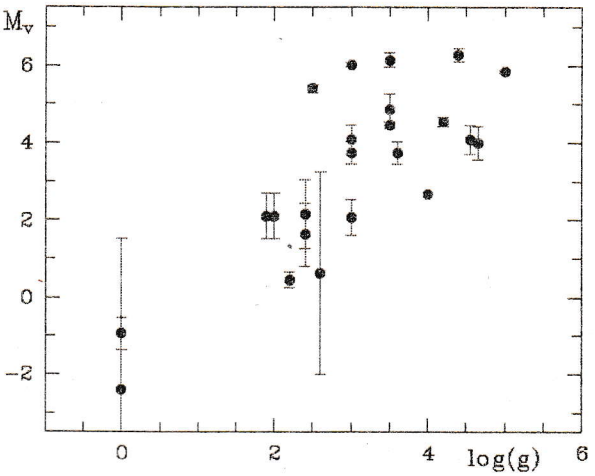

Figure 5: *Absolute magnitude* M_V *calculated using Hipparcos parallaxes vs. log g here determined.*

4.1. Light elements

Following the usual practice, we include Na, Mg, Al, Si, S, Ca and Ti in this group of elements ($11 \leq Z \leq 22$). The elements of this group, having even-numbered Z, are synthesized in α-process reactions. They may be produced in stars of any metallicity, whereas the synthesis of the odd Z elements depends on neutron excess (and thus on metallicity) in the regions of nuclear reactions (Wheeler et al., 1989). Let us consider these two groups separately.

α-process elements. In Fig. 6a is shown the relationship between the averaged abundance of all, but for sulphur, elements of this group measured for each star and its metallicity. Beginning from the approximately solar metallicity to the most metal-deficient stars, one can well trace the excess in the ratio [α/Fe]. Despite the scatter of points, our data are, on the whole, in good agreement with the data of other researchers: an approximately constant abundance at the level of +0.5 dex in the range of metallicities $-3 \leq$ [Fe/H] ≤ -1.4 and a gradual drop to zero with increasing metallicity to the level of solar. For the above range of metallicities the following excesses are characteristic of this group of elements: [Mg/Fe] = +0.59 dex, [Si/Fe] = +0.66 dex, [Ca/Fe] = +0.33 dex, [Ti/Fe] = +0.42 dex. The relationship between the abundance and metallicity for each element replicates on the whole the relationship derived from averaging the abundances of all α-process elements, although for Si an overabundance of $\approx$ 1 dex has been found for two most low metallicity

Table 2: *Relative abundances [X/Fe] of chemical elements in the atmospheres of the stars investigated*

	G 30-52	G 126-62	G 170-47	G 231-52	G 245-32
Na1	0.45(0.08)(6)	0.21(0.04)(6)	-	-	-0.46(0.14)(3)
Mg1	0.43(0.14)(4)	-0.15(0.03)(4)	0.74(0.27)(4)	0.06(0.00)(1)	0.41(0.10)(4)
Al1	-0.02(0.07)(4)	0.08(0.08)(4)	-	-	0.21(0.17)(4)
Si1	0.03(0.06)(24)	0.25(0.06)(10)	-	0.70(0.24)(2)	0.28(0.03)(17)
Si2	-0.05(0.00)(1)	0.26(0.00)(1)	-	-	-
S1	1.23(0.16)(4)	0.42(0.08)(6)	2.11(0.07)(5)	1.52(0.15)(5)	0.87(0.10)(6)
Ca1	0.06(0.07)(13)	0.32(0.03)(19)	0.24(0.02)(12)	0.12(0.05)(15)	-0.12(0.05)(21)
Ca2	-	-	-	-	-
Sc2	-	0.04(0.06)(4)	-0.41(0.00)(1)	0.04(0.00)(1)	0.06(0.10)(6)
Ti1	-0.08(0.06)(21)	0.52(0.04)(9)	0.11(0.07)(4)	0.59(0.05)(3)	-
Ti2	-	0.60(0.04)(7)	0.05(0.05)(5)	-	-
V1	-0.11(0.04)(12)	1.38(0.05)(6)	-	-	1.50(0.08)(14)
V2	-	1.18(0.00)(2)	-	-	0.82(0.12)(4)
Cr1	-0.08(0.07)(6)	0.10(0.05)(4)	-0.24(0.13)(2)	-0.05(0.04)(4)	-
Cr2	-	0.17(0.09)(3)	-	-	-
Mn1	-0.22(0.09)(4)	-	-	-	-0.50(0.09)(2)
Fe1	0.00(0.01)(35)	0.00(0.02)(55)	0.00(0.01)(52)	0.00(0.02)(43)	0.00(0.02)(37)
Fe2	-0.02(0.04)(9)	0.01(0.03)(11)	0.00(0.04)(8)	0.01(0.07)(8)	-0.01(0.09)(9)
Ni1	-0.40(0.06)(20)	0.04(0.04)(7)	0.00(0.06)(3)	0.16(0.05)(4)	0.45(0.05)(13)
Cu1	-	0.20(0.05)(3)	-	-	-
Zn1	-	-	-	-	0.61(0.00)(1)
Y2	0.09(0.00)(1)	-	-	-	-
Zr2	-	-	-	-	-
Ba2	-0.25(0.15)(2)	0.21(0.10)(3)	-0.88(0.01)(2)	-0.04(0.11)(3)	-0.24(0.14)(3)
La2	-0.30(0.27)(4)	-	-	-	-
Ce2	-	-	-	-	-
Pr2	-	-	-	-	-
Nd2	0.37(0.00)(1)	-	-	-	-
Eu2	0.76(0.00)(1)	-	-	-	-

Table 2: *Continued*

	HD 65583	HD 88609	HD 175305	BD 09°3223	BD 11°2998
Na1	-0.02(0.03)(4)	-	-0.17(0.04)(4)	0.24(0.33)(3)	-
Mg1	0.34(0.08)(6)	0.69(0.03)(4)	0.18(0.07)(4)	-0.11(0.08)(4)	0.33(0.05)(6)
Al1	0.08(0.04)(3)	-	0.05(0.00)(1)	-	-
Si1	0.12(0.03)(18)	1.15(0.06)(6)	0.19(0.02)(13)	0.85(0.02)(12)	0.42(0.02)(13)
Si2	-0.08(0.00)(1)	1.02(0.00)(1)	0.09(0.00)(1)	-	0.51(0.00)(1)
S1	-0.41(0.14)(3)	2.35(0.07)(7)	0.75(0.05)(6)	1.09(0.08)(3)	0.23(0.17)(4)
Ca1	0.10(0.03)(19)	0.34(0.02)(15)	0.26(0.03)(18)	0.19(0.04)(13)	0.24(0.04)(19)
Ca2	-	-	-	-	-
Sc2	0.18(0.04)(6)	-0.32(0.04)(3)	-0.11(0.02)(8)	0.13(0.04)(7)	0.04(0.05)(8)
Ti1	0.36(0.03)(16)	0.01(0.04)(9)	0.16(0.02)(22)	0.67(0.02)(15)	0.23(0.05)(14)
Ti2	0.38(0.00)(1)	0.05(0.03)(7)	0.15(0.04)(9)	0.18(0.04)(9)	0.31(0.03)(8)
V1	0.37(0.02)(15)	-	-0.05(0.03)(10)	1.22(0.03)(6)	0.12(0.05)(6)
V2	0.42(0.00)(1)	-	-	1.38(0.05)(2)	0.10(0.02)(2)
Cr1	0.13(0.05)(10)	-0.38(0.03)(5)	-0.16(0.04)(9)	-0.04(0.06)(6)	0.00(0.04)(7)
Cr2	-	-	0.04(0.05)(4)	-0.03(0.07)(3)	-0.12(0.04)(7)
Mn1	-0.04(0.03)(3)	-	-0.48(0.03)(5)	0.50(0.07)(5)	-0.26(0.00)(5)
Fe1	0.00(0.01)(64)	0.00(0.01)(34)	0.00(0.01)(72)	0.00(0.01)(36)	0.00(0.01)(76)
Fe2	-0.02(0.05)(7)	0.01(0.03)(14)	0.00(0.02)(16)	-0.02(0.04)(8)	0.01(0.04)(17)
Ni1	-0.02(0.03)(18)	0.04(0.06)(4)	-0.12(0.02)(28)	0.26(0.04)(12)	0.02(0.04)(17)
Cu1	0.14(0.00)(1)	-0.40(0.00)(1)	-0.56(0.02)(2)	-	-0.30(0.04)(3)
Zn1	-	0.32(0.00)(1)	-0.02(0.02)(3)	-	-0.01(0.00)(1)
Y2	0.36(0.03)(2)	-0.33(0.01)(3)	-0.05(0.04)(5)	-0.06(0.04)(3)	-0.14(0.03)(5)
Zr2	-	-	0.06(0.00)(1)	-	0.44(0.09)(3)
Ba2	0.25(0.08)(3)	-1.03(0.00)(3)	0.32(0.10)(3)	-0.15(0.10)(3)	0.30(0.06)(3)
La2	0.50(0.06)(3)	-	0.10(0.11)(3)	-	0.15(0.04)(4)
Ce2	-	0.15(0.02)(3)	-0.05(0.04)(5)	-	0.61(0.03)(2)
Pr2	-	-	0.45(0.02)(2)	-	0.23(0.07)(2)
Nd2	-	-	0.19(0.04)(7)	-	-0.22(0.02)(4)
Eu2	-	0.76(0.07)(2)	0.49(0.01)(2)	-	0.33(0.01)(2)

Table 2: *Continued*

	BD 17°3248	BD 23°3912	HD 122563	α CMi
Na1	-0.01(0.16)(3)	-0.15(0.05)(2)	0.47(0.06)(2)	0.22(0.06)(5)
Mg1	0.23(0.07)(3)	0.36(0.08)(5)	0.51(0.06)(5)	-0.04(0.03)(5)
Al1	-	0.39(0.05)(3)	-	0.04(0.11)(3)
Si1	0.43(0.03)(9)	0.37(0.06)(9)	0.91(0.06)(8)	0.06(0.03)(28)
Si2	0.34(0.00)(1)	0.25(0.00)(1)	0.82(0.00)(1)	0.03(0.06)(2)
S1	0.81(0.04)(3)	1.47(0.10)(3)	1.70(0.05)(7)	-0.07(0.05)(6)
Ca1	0.07(0.06)(10)	0.33(0.03)(25)	0.40(0.02)(18)	0.11(0.05)(20)
Ca2	-	-	-	0.12(0.06)(2)
Sc2	-0.26(0.04)(9)	-0.11(0.06)(5)	-0.27(0.02)(6)	-0.11(0.05)(4)
Ti1	-0.01(0.06)(8)	0.40(0.05)(10)	0.06(0.04)(12)	0.13(0.04)(15)
Ti2	0.20(0.10)(7)	0.29(0.06)(7)	-0.05(0.04)(9)	-0.01(0.06)(8)
V1	0.86(0.02)(6)	0.85(0.06)(11)	0.65(0.06)(10)	0.07(0.09)(6)
V2	1.01(0.00)(1)	1.25(0.09)(3)	0.60(0.02)(2)	-0.18(0.10)(4)
Cr1	0.09(0.08)(7)	-0.00(0.04)(7)	-0.35(0.04)(5)	0.03(0.04)(15)
Cr2	0.13(0.07)(5)	0.11(0.06)(2)	0.02(0.11)(3)	-0.14(0.05)(7)
Mn1	-	0.13(0.07)(6)	-0.12(0.07)(3)	0.06(0.04)(9)
Fe1	0.00(0.02)(47)	0.00(0.01)(72)	0.00(0.01)(44)	0.00(0.01)(77)
Fe2	-0.02(0.06)(11)	0.01(0.04)(16)	0.01(0.05)(12)	0.01(0.02)(22)
Ni1	-0.19(0.03)(16)	0.04(0.05)(13)	0.20(0.05)(14)	0.01(0.02)(28)
Cu1	0.17(0.05)(2)	0.04(0.18)(2)	-0.05(0.51)(2)	0.21(0.12)(3)
Zn1	-	-	0.14(0.03)(2)	-0.14(0.02)(2)
Y2	0.24(0.03)(3)	-0.02(0.03)(2)	-0.77(0.03)(2)	-0.18(0.04)(4)
Zr2	-0.00(0.08)(3)	0.44(0.08)(3)	-	-0.11(0.33)(2)
Ba2	-	0.03(0.10)(3)	-1.18(0.03)(3)	0.20(0.12)(3)
La2	-	-	0.33(0.02)(3)	-
Ce2	-	0.62(0.07)(4)	0.38(0.02)(3)	-0.15(0.00)(1)
Pr2	-	-	0.65(0.02)(2)	-
Nd2	0.53(0.07)(4)	-	0.73(0.01)(2)	-0.06(0.02)(4)
Eu2	0.86(0.02)(2)	-	0.62(0.02)(2)	0.21(0.18)(2)

stars, while Ti, on the contrary, shows the solar abundance for these two stars. The data of other authors (Gratton and Sneden, 1991; Magain, 1989 for titanium and Gratton and Sneden, 1988; Magain, 1987 for silicon) are consistent with ours, although Si from their results does not exceed 0.85 dex, while the Ti abundance does not fall below 0.2 dex for the most metal-deficient stars.

When determining the mean abundance of α-process elements, sulphur was disregarded; this was primarily due to the large spread of the results obtained and overabundances amounting to ≈ 2 dex for the most metal-poor stars of our sample (see Fig. 6b). This may partly be due to the insufficiently accurate oscillator strengths we have used in the calculations as well as to the large errors in the equivalent widths of the measured lines, which is first of all associated with the weakness of lines in the spectra of the stars studied.

Odd Z elements Na and Al. The [Al/Fe] and [Na/Fe] ratios span a range of approximately 1 dex (Fig. 6c, open and filled symbols, respectively) with a large dispersion in the interval of metallicity of $-3 <$ [Fe/H] < 0 dex. There is a small overabundance of +0.11 and +0.06 dex for the averaged abundances of [Al/Fe] and [Na/Fe], respectively. The two elements, as well as magnesium, are nearly completely synthesized in massive stars and get to the interstellar medium with second-type supernova outbursts. Therefore one may expect the abundance of Na and Al to be correlated with that of Mg. On the other hand, the Na and Al synthesis is also dependent on the neutron excess (hence on metallicity). Thus a relation of the type $[\mathrm{Na,\ Al/Mg}] = \alpha[\mathrm{Mg/H}] + \mathrm{const}$ may be suggested, where $\alpha \geq 0$ (Nissen and Schuster, 1997). Fig. 7 shows the relationship between the abundances of odd–Z elements, Na and Al, relative to α–elements [Na,Al/α] and the abundance of α–elements [α/H]. The best straight–line fit to the data on dwarf stars is $[\mathrm{Na,Al}/\alpha] = 0.21\ [\alpha/\mathrm{H}] - 0.16$ and to the data on other stars is $[\mathrm{Na,Al}/\alpha] = 0.17[\alpha/\mathrm{H}] + 0.08$.

4.2. Iron group elements

This group includes Cr, Mn, Fe, Ni, lighter elements Sc, Ti, and heavier elements Cu and Zn. Abundances of some iron peak elements (Cr, Sc and Cu) are summarized in Fig. 8a–c. The abundances of Sc, Mn and Ni correspond to that of iron: the mean values are $[\mathrm{Sc/Fe}] = -0.07$ dex, $[\mathrm{Mn/Fe}] = -0.01$ dex and $[\mathrm{Ni/Fe}] = +0.02$ dex. In the metallicity range $-1.4 \leq$[Fe/H]≤ 0 chromium follows after iron; at lower metallicities it is observed to be slightly deficient. The abundances of Cu and Zn were estimated only from two–three lines accessible to measurement. This, apparently, accounts for the great spread of the

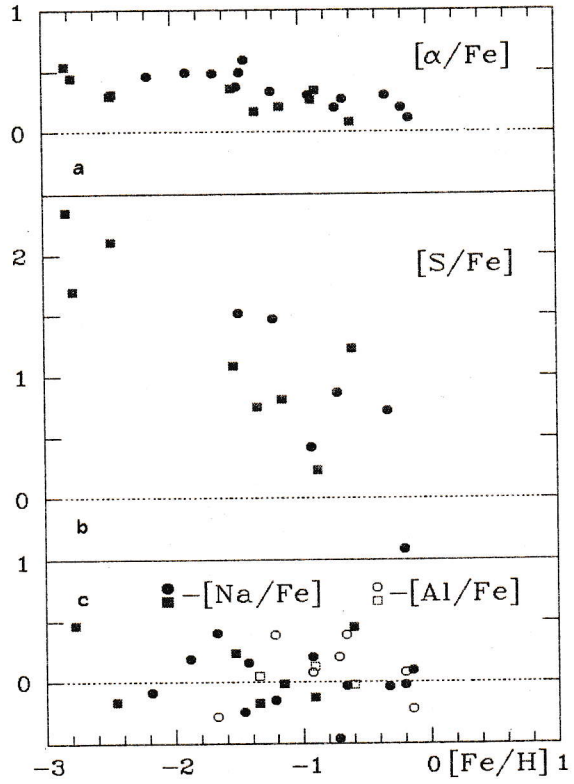

Figure 6: *Even– and odd–Z light element abundance trends; (a) averaged abundance of Mg, Si, Ca, and Ti relative to iron; (b) sulphur; (c) sodium and aluminium. The data for stars with* $\log g \geq 3$ *are denoted by circles, with* $\log g < 3$ *– by squares.*

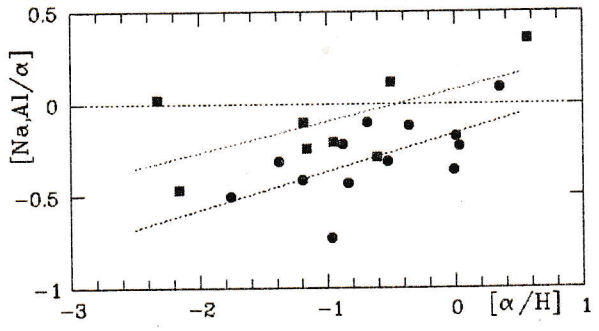

Figure 7: *[Na,Al/α] vs. [α/H] with the same symbols as used in Fig. 6.*

data obtained, especially for Zn. Nevertheless, it can be stated with any assurance that [Cu/Fe] increases gradually from ≈ -0.25 dex to zero with growing metallicity. Zinc is likely to be observed in excess throughout the whole range of metallicities: the mean [Zn/Fe] = +0.22 dex.

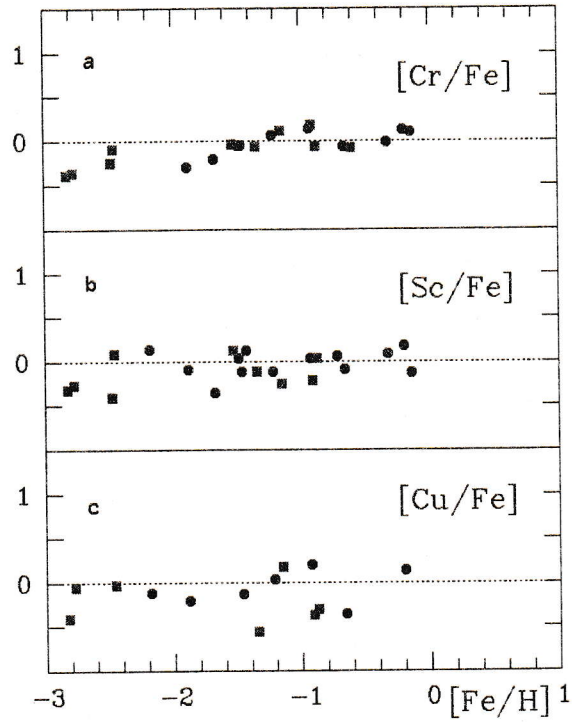

Figure 8: *Abundances of iron group elements as a function of metallicity [Fe/H]; symbols used are the same as in Fig. 6.*

4.3. s- and r-process elements

The elements of this group are synthesized in the processes of neutron capture: in the reactions of r-process, if the time of neutron capture is comparable with the time of β-decay, and of s-process, if addition of neutrons occurs by several orders of magnitude slower. All these elements are synthesized in the reactions of both s- and r-processes but such elements as Y and Ba are synthesized mainly in the s-process, whereas Eu — in the r-process (Gratton and Sneden, 1994). Since these two processes take place predominantly in the course of evolution of stars of different masses, the abundance of the elements of this group is of prime importance in the construction of the chemical evolution model of the Galaxy.

Our results for heavy element abundances are summarized in Fig. 9a–c. Here "s–process" means the averaged abundances of Y, Zr and Ba, and "lanthanoides" means the averaged abundances of La, Ce, Pr, and Nd. Determination of the heavy metal abundances is particularly impeded due to the small number of lines suitable for analysis. In the case of metal–poor stars the situation is additionally complicated by the fact that because of the low metallicity, the lines of these metals are very weak. Fig. 9a indicates

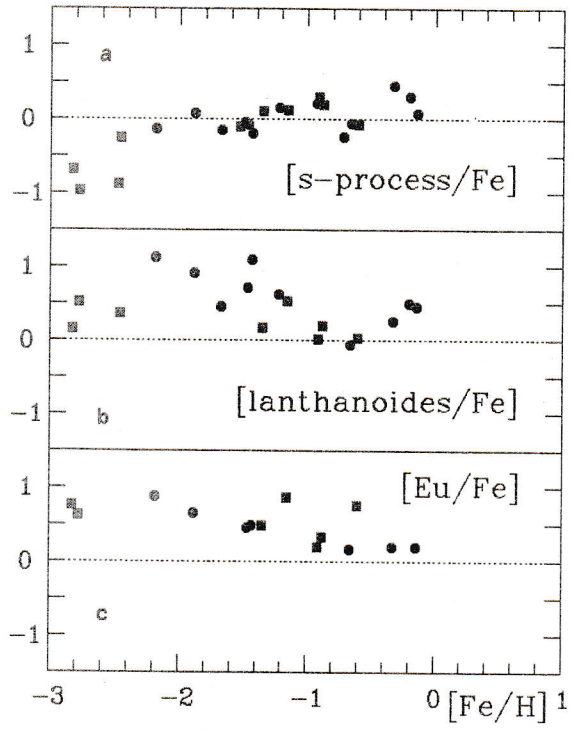

Figure 9: *Heavy element abundance trends; (a) averaged abundances of Y, Ba and Zr; (b) averaged abundances of La, Ce, Pr and Nd; (c) Eu; symbols used are the same as in Fig. 6.*

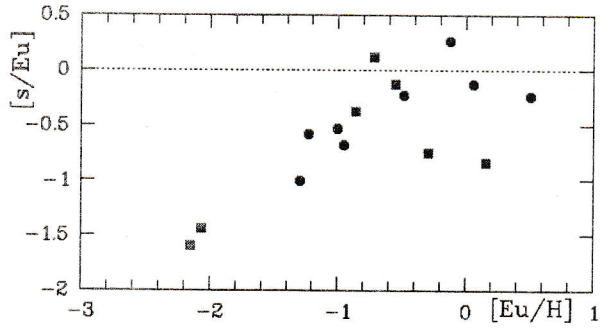

Figure 10: *[s/Eu] vs. [Eu/H]; symbols used are the same as in Fig. 6.*

that the s–process elements abundance is close to the solar value in the range $-2.2 < [Fe/H] < 0$ dex, the average value [s/Fe] = 0.04 dex; while for extremely metal–poor stars the quantity [s/Fe] decreases to very low values.

The average abundances of lanthanoides (Fig. 9b) increases with dropping metallicity in the interval from 0 to −2 dex and then drops to the approximately solar value for most metal–poor stars. The [Eu/Fe] ratio initially rises as metallicity declines and then, probably, is constant in the metallicity range $-3 < [Fe/H] < -2$ dex (Fig. 9c).

Fig. 10, where the abundance of s–process elements relative to Eu, [s/Eu], is shown vs. [Eu/H], suggests that Eu is a pure r–process element. The enhancement of s–process with respect to europium (Fig. 10) when passing from the stars of extreme halo population to objects of the old disk agrees well with the general scheme that the s-process is more important, as compared to the r-process, with approaching the phase of galaxy disk formation.

5. Conclusions

The paper presents new results on the chemical composition of the halo population obtained on the basis of high-resolution echelle spectra. The parameters of stellar atmospheres determined from spectroscopy data alone are generally different from those based on photometry. The effective temperature and metallicity turn out to be systematically higher; the part of stars classified as halo subdwarfs from photometry data most likely belong to halo and disk supergiants.

References

Bartkevičius A., 1980, Bull. Viln. Astr. Obs., **51**
Carney B.W., Latham D.W., Laird J.B. et al., 1994, Astron. J., **107**, 2240
Edvardsson B., Andersen J., Gustafsson B., Lambert D.L., Nissen P.E., Tomkin J., 1993, Astron. Astrophys., **275**, 101
Galazutdinov G.A., 1992, SAO Preprint, **92**
Gratton R.G., Sneden C., 1988, Astron. Astrophys., **204**, 193
Gratton R.G., Sneden C., 1991, Astron. Astrophys., **241**, 501
Gratton R.G., Sneden C., 1994, Astron. Astrophys., **287**, 927
Grevesse N., Noels A., Sauval A.J., 1996, ASP Conf. Ser. **99**, 117
Iben I., 1983, Ann. Rev. Astron. Astrophys., **21**, 271
Klochkova V.G: 1995, SAO Report, **259**, 1
Klochkova V.G., Panchuk V.E., 1996, Astron. Rep., **73**, 912
Klochkova V.G., Mal'kova G.A., Panchuk V.E., 1996, Bull. Spec. Astrophys. Obs., **39**, 5
Kurucz R.L., 1993, CDROM N13
Magain, P., 1987, Astron. Astrophys., **179**, 176
Magain, P., 1989, Astron. Astrophys., **209**, 211
Nissen P.E., Schuster W.J., 1997, Astron. Astrophys., **326**, 751
Panchuk V.E, Najdenov I.D, Klochkova V.G, Ivanchik A.B., Yermakov S.V, Murzin V.A., 1998, Bull. Spec. Astrophys. Obs., **44**, 127
Steffen M., 1985, Astron. Astrophys. Supl. Ser., **59**, 403
Truran W.J, 1984, Ann. Rev. Nucl. Part. Sci., **34**, 53
Wheeler J.C., Sneden C., Truran W.J., 1989, Ann. Rev. Astron. Astrophys., **27**, 279
Woosley S.E., Weaver T.A, 1986, Ann. Rev. Astron. Astrophys., **24**, 205